Hybrid Beamforming Optimization for UAV-Enabled mmWave Beamspace MIMO System

Zhen Chen*, Jie Tang*, Hengbin Tang*, Xiuyin Zhang* Daniel Ka Chun So‡, Nan Zhao† and Kai-Kit Wong§

*School of Electronic and Information Engineering, South China University of Technology, Guangzhou, China,
†School of Information and Communication Engineering, Dalian University of Technology, Dalian, China,
‡School of Electrical and Electronic Engineering, University of Manchester, Manchester, United Kingdom, UK,
§Department of Electronic and Electrical Engineering, University College London, UK
E-mail:chenz@scut.edu.cn; eejtang@scut.edu.cn; zhangxiuyin@scut.edu.cn

Abstract—The combination of unmanned aerial vehicles (UAVs) and millimeter wave (mmWave) multiple-input multiple-out (MIMO) systems is considered as a key enabling technology for 5G networks, as it provides high data rate aerial links. However, establishing UAV-enabled mmWave MIMO communication is challenging duo to the high hardware cost in terms of radio frequency (RF) chains. As explored in this work, the joint optimization of the UAV's altitude and hybrid beamspace precoding is proposed for the UAV-enabled multiuser MIMO system, in which the discrete lens arrays (DLA) is exploited to decrease the amount of the RF chain. In the proposed scheme, the optimization problem is formulated as a minimum weighted mean squared error (MWMSE) method. Then an efficient algorithm with the penalty dual decomposition is proposed to optimize the altitude of UAV, selection of the beam and the method of digital precoding jointly. Simulation results confirm the superior performance of the explored scheme and perform close to full-digital beamforming in terms of achievable spectral efficiency.

Index Terms—UAV, mmWave communication, MIMO, hybrid beamspace precoding, lens antenna arrays.

I. INTRODUCTION

Unmanned aerial vehicles (UAVs) have been widely used in both military and commercial applications and can be enhanced by multiple-input-multiple-output (MIMO) for wireless communication networks. Different from conventional terrestrial communications, UAVs can construct an ondemand scalable platform for the deployment of aerial base stations, or mounting mobile access points (APs) [1]. Due to the flexibility and mobility, UAVs can act as flying base stations (BSs) to provide temporary or urgent support, which enhances the wireless capacity for ground terminals (GTs). Particularly, UAVs are used to provide various services, such as sampling data from dangerous areas, firefighting and disaster rescue [2]. In addition, UAVs are envisioned to be a prime candidates of future mmWave communication systems [3]. Because of the short wavelength at mmWave frequency, massive antenna arrays can be deployed on a UAV to form the beam-steerable directive beam, which is witnessed as a promising approach for offering available data rates and extensive coverage [4].

However, the conventional mmWave MIMO system mostly applies the fully digital precoding, where one dedicated radio frequency (RF) chain is required by each antenna usually [5]. As a result, high hardware and energy cost is resulted, which obstruct the commercial deployment of mmWave MIMO systems [6]. Even worse, the RF components may cost up to 70% of the total transceiver energy consumption [5]. Therefore, the demand on radio frequency (RF) chains makes the UAV-enabled mmWave Massive MIMO system unrealistic to low-cost communications.

To tackle this challenge, lots of studies have been developed in order to reduce the energy cost and the number of RF chains, such as load-controlled parasitic antenna arrays (LC-PAAs) [7], beam selection [8]–[10] and hybrid analog/digital precoding design [11]. The recent concept of "*beamspace MIMO*" has been exploited as a potential scheme to substantiality reduce the hardware cost of RF chains, where the discrete lens array (DLA) is considered for analog spatial beamforming [12]. In beamspace MIMO systems, the electromagnetic (EM) lens with the antenna array are developed for analog spatial beamforming domain [13], [14]. To compensate the high attenuation of mmWave frequencies, the different directions of mmWave signals can be focused on the antenna array, which is referred to as *beamspace channel* [15]. As a result of the high path loss on mmWave frequencies, the beamspace mmWave channel with lens antenna array (LAA) is sparse, meaning that only a part of beams carry the majority of the information. Thus the method for beam selection will be designed to pick out a few energy-focusing beams, which will reduce the demanded number of RF chains with only a negligible performance degradation [17]. However, these works are restricted to the terrestrial communications, where the beam selection techniques developed for mmWave MIMO systems primarily considered a static or quasi-static scenario. Due to the fragility to emergency (e.g., natural disasters, sudden gathering), the recovery demand of communication will be extremely fast which will be unrealistic for fixed networks. Therefore, that is important to develop a beam selector and beamspace precoding method for UAV-enabled
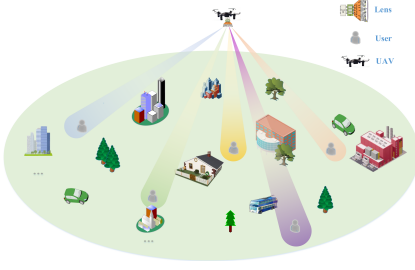
Fig. 1. Illustration of the mmWave MIMO system with lens antenna array.

mmWave beamspace MIMO systems.

Motivated by the aforementioned observations, this work investigates the joint optimal beam selector and precoding method for UAV-enabled mmWave MIMO system. The joint optimization problem is NP-hard, which makes the formulated hybrid beamforming (HBF) problem non-trivial to solve. To tackle this problem, the optimization problem is reformulated as equivalent augmented Lagrangian (AL) function, where each subproblem is solved independently using the block co-ordinate descent (BCD) algorithm. Simulation results validate the practicality of the proposed strategy.

The organization of the remaining paper follows. Section II presents the model of the multi-user mmWave beamspace system model along with the joint optimization problem formulation. We explain the optimization procedure in Section III. In Section IV, the simulations are provided to validate the theoretical findings, followed by the conclusions in Section V.

Notations: scalars are denoted by lower-case letters; lower-case and upper-case boldface letters are used for vectors and matrices, respectively; $\mathrm{tr}(\cdot)$ is the trace of a matrix; $\log_2(\cdot)$ is used for the base two logarithm; The superscripts $(\cdot)^T$, $(\cdot)^H$, denote the transpose and conjugate transpose, respectively; $\mathbf{x}^H$ is the conjugate of a complex signal $\mathbf{x}$; $(\cdot)_j$ and $(\cdot)_{i,j}$ represent the i-th column and i-th row and j-th column element of a matrix, respectively; $\|\cdot\|_2$, $\|\cdot\|_F$ and $\mathrm{diag}(\cdot)$ denote the Euclidean nrom, Frobenius norm and diagonalization operators.

II. PROBLEM FORMULATION

The downlink of mmWave MIMO system is described, where a UAV is deployed as a flying BS to serve K simulta-neous GTs in Fig.1. The UAV-BS is equipped with LAAs, and the LAA owns a few of RF chains, however, the number of RF chains is less than the antenna number. We assume that the UAV-BS with horizontal and vertical location $\mathbf{z} = (z(1), z(2))$ is hovering at altitude of h meters above the ground level. We assume that the height of each GT is zero compared with the height of the UAV-BS. The UAV-BS with N_t transmit antennas and N_t^{RF} chains serves a total of K GTs each of which is equipped with N_r receive antennas. It is assumed that N_s data streams are transmitted to a receiver, which are subject to constraints $KN_s \leq N_t^{RF} \ll N_t$ and $N_s \leq N_r$.

Owing to the sparsity and high path loss of free-space at mmWave band, we consider the channel model as a Rician fading model. Different from the conventional low frequency channels, the mmWave channels between UAV and GTs are stochastic fading, and the channel matrix from the k-th GT to the UAV can be expressed as [18]

$$\hat{\boldsymbol{H}}_k = \sqrt{\beta_0(d_k)^{-\alpha}} \left(\sqrt{\frac{\delta}{\delta+1}} G_k + \sqrt{\frac{1}{\delta+1}} \hat{G}_k \right), \quad (1)$$

where β_0 is the channel power gain, $d_k = \sqrt{\|\mathbf{z} - \mathbf{x}_k\|_2^2 + h^2}$ is the distance between the UAV and GT k and $\alpha \geq 2$ is the path loss exponent. G_k is the LoS component of the GT k with $G_k(i,j) = 1$; $\hat{G}_k$ denotes the the Rayleigh fading channel (or NLoS) component of the GT k and $\delta \geq 0$ is the Rician factor specifying the power ratio.

A. The Lens-Aided mmWave MIMO Systems

By using the combination of a lens and a uniform linear arrays (ULA) of antennas, the signals emitted from various unknown directions will be gathered on different positions of a ULA, the signals is reflected by lens. The lens can be modelled as a spatial-domain discrete Fourier transform (DFT) matrix $\mathbf{U}$, the array steering vectors of N_t directions covering the whole space can be described as follows [19]

$$\mathbf{U} = \left[\mathbf{a}(\overline{\phi}_1), \mathbf{a}(\overline{\phi}_2), ..., \mathbf{a}(\overline{\phi}_{N_t}) \right]^H, \quad (2)$$

where $\mathbf{a}(\overline{\phi})$ is the steering vector for the spatial direction $\overline{\phi}$. Thus, the physical spatial MIMO channel $\hat{\mathbf{H}}_k$ in (1) can be derived as the beamspace channel with a precisely designed lens antenna arrays, which is defined as [12]

$$\tilde{\mathbf{H}}_k = \hat{\mathbf{H}}_k \mathbf{U} \quad (3)$$

For each GT, the received signal is first processed with a digital combiner $\mathbf{V}_k \in \mathbb{C}^{N_s \times N_r}$. Let $\mathbf{H}_k = (\|\mathbf{z} - \mathbf{x}_k\|_2^2 + h^2)^{\frac{\alpha}{2}} \tilde{\mathbf{H}}_k$, the received signal of GT k can be simplified as

$$\mathbf{y}_k = \left(\|\mathbf{z} - \mathbf{x}_k\|_2^2 + h^2 \right)^{-\frac{\alpha}{2}} \mathbf{V}_k^H \mathbf{H}_k \mathbf{S} \mathbf{W} \mathbf{c} + \mathbf{V}_k^H \mathbf{n}_k \quad (4)$$

where $\mathbf{W} = [\mathbf{W}_1, \mathbf{W}_2, ..., \mathbf{W}_K] \in \mathbb{C}^{N_t^{RF} \times KN_s}$ is the digital precoder, $\mathbf{c} = [c_1^T, c_2^T, ..., c_K^T]^T \in \mathbb{C}^{KN_s \times 1}$ is the transmitted signal vector for K GTs. $\mathbf{n} \sim \mathcal{CN}(0, \sigma^2)$ is additive white Gaussian noise (AWGN) and $\mathbf{S} \in \mathbb{C}^{N_t \times N_t^{RF}}$ is used for the beam selection matrix, as a characterization matrix, the entries $s_{i,j}$ of the matrix are either 0 or 1.

B. Hybrid Beamforming Optimization Problem Formulation

According to (4), the hybrid beamspace beamforming de-sign is to maximize sum-rate, which can be formulated as

$$\max_{\mathbf{W}, \mathbf{S}, h, \mathbf{z}} \sum_{k=1}^{K} \log_2 \det \left(\mathbf{I} + \frac{\mathbf{H}_k \mathbf{S} \mathbf{W} \mathbf{W}^H \mathbf{S}^H \mathbf{H}_k^H}{\sigma^2(\|\mathbf{z} - \mathbf{x}_k\|_2^2 + h^2)^\alpha} \right) \quad (5a)$$

$$s.t. \quad \mathrm{tr}\left(\boldsymbol{S} \boldsymbol{W}_k \boldsymbol{W}_k^H \boldsymbol{S}^H \right) \leq P, \quad (5b)$$

$$\sum_{i=1}^{N_t} s_{i,j} = 1, \quad \sum_{j=1}^{N_t^{RF}} s_{i,j} \leq 1, \quad s_{i,j} \in \{0,1\} \quad (5c)$$

$$h_{\min} \leq h \leq h_{\max} \quad (5d)$$

639

where P_k is the maximum transmit power at the k-th GT, $[h_{\min}, h_{\max}]$ is the feasible region of height h determined by obstacle heights and authority regulations of UAVs. The constraints $\sum_{i=1}^{N_t} s_{i,j} = 1, j = 1, 2, ..., N_r^{RF}$, guarantee that every RF chain can be fed a single beam, while the constraints $\sum_{j=1}^{N_r^{RF}} s_{i,j} \leq 1, i = 1, 2, ..., N_t$ ensure that every beam can be chosen for no more than one RF chain.

It is worth mentioning that the optimization problem (5) involves a joint optimization over four variables, along with non-convex constraints. To obtain an effective algorithm for problem (5), the equivalent optimization problem (5) is proposed that this problem can be rewritten into a simpler form by taking the modified MMSE [20]. Inspired by MMSE criterion, let $C_k^{(n)} = \hat{\mathbf{E}}_k^{-1}$ denoting the previous iteration of result and $D_k = \|\mathbf{z} - \mathbf{x}_k\|_2^2$, the hybrid beamforming design problem (5) is equivalent to the following problem

$$\min_{\mathbf{W}, \mathbf{V}_k^H, \mathbf{S}, h, \mathbf{z}} \sum_{k=1}^{K} \operatorname{tr}\left(C_k^{(n)} \mathbf{E}_k\right) \tag{6a}$$

$$s.t. \quad \operatorname{tr}\left(\boldsymbol{S} \boldsymbol{W}_k \boldsymbol{W}_k^H \boldsymbol{S}^H\right) \leq P, \tag{6b}$$

$$\sum_{i=1}^{N_t} s_{i,j} = 1, \quad \sum_{j=1}^{N_t^{RF}} s_{i,j} \leq 1 \quad s_{i,j} \in \{0, 1\}, \tag{6c}$$

$$h_{\min} \leq h \leq h_{\max}. \tag{6d}$$

Therefore, the sum-rate optimization problem (5) can be transformed into a weighted MSE minimization problem (6). As following, an efficient BCD algorithm will be studied to address the equivalent problem (6) in the next section.

III. PROPOSED HYBRID BEAMFORMING DESIGN

In this section, we turn our attention to solve the problem (6), which is divided into a series of sub-problems: altitude of UAV h, location $\mathbf{z}$, digital combiner $\mathbf{V}_k^H$, digital precoder $\mathbf{W}$, beam selector $\mathbf{S}$ and solve each independently. The specific procedures are summarized as follows.

A. Optimal Altitude of UAV

We investigate the altitude planning of UAV with fixed $\boldsymbol{W}$, $\boldsymbol{V}_k^H$ and $\boldsymbol{S}$. Then, the optimization problem (6) is formulated as

$$\min_{h} \sum_{k=1}^{K} (h \mathbf{sec}\Theta)^{-2\alpha} A_k - (h \mathbf{sec}\Theta)^{-\alpha} B_k + C_k, \tag{7a}$$

$$s.t. \qquad h_{\min} \leq h \leq h_{\max}, \tag{7b}$$

where $A_k = \operatorname{tr}\left(\xi_k \boldsymbol{V}_k^H \boldsymbol{H}_k \boldsymbol{S} \boldsymbol{W} \boldsymbol{W}^H \boldsymbol{S}^H \boldsymbol{H}_k^H \boldsymbol{V}_k\right)$, $B_k = -2\operatorname{tr}\left(\boldsymbol{V}_k^H \boldsymbol{H}_k \boldsymbol{S} \boldsymbol{W}\right)$, $C_k = \left[\sigma^2 \operatorname{tr}\left(\xi_k \boldsymbol{V}_k^H \boldsymbol{V}_k\right) + \xi_k \boldsymbol{I}_{N_s}\right]$.

Based on (7), defining function $f(\boldsymbol{x}(h)) \triangleq A_k \boldsymbol{x}^2(h) - B_k \boldsymbol{x}(h) + C_k$ and $\boldsymbol{x}(h) \triangleq (h \mathbf{sec}\Theta)^{-\alpha}$, we have

$$f'(\boldsymbol{x}(h)) = 2A_k \boldsymbol{x}(h) - B_k \tag{8}$$

It follows that the optimal altitude of UAV is obtained in the following two cases.

1) Case 1: If $\boldsymbol{x}(h) > \frac{B_k}{2A_k}$, we have $f'(\boldsymbol{x}(h)) > 0$, and $f(\boldsymbol{x}(h))$ is an monotonically increasing function when $\hat{h}_{\min} \leq h \leq h_{\max}$. The optimal value of h is denoted by h^* and observing that the $\boldsymbol{x}(h)$ is monotonic decreasing with h, which yields

$$h^* = h_{\max}. \tag{9}$$

2) Case 2: If $\boldsymbol{x}(h) \leq \frac{B_k}{2A_k}$ and $\hat{h}_{\min} \leq h \leq h_{\max}$, $f(\boldsymbol{x}(h))$ is a monotonically decreasing function. The optimal $\boldsymbol{x}(h)^*$ is

$$h^* = h_{\min}. \tag{10}$$

After the flight altitude h^* is obtained, a 2D exhaustive search is used to achieve the optimal location planning $\mathbf{x}$ of UAV to the optimization problem (7).

B. Hybrid Beamspace Beamforming Design

Now we turn our attention to optimize $\mathbf{W}$, $\mathbf{V}_k^H$, $\mathbf{S}$ simultaneously by fixing the other variables. Let $\overline{\mathbf{H}}_k = \left(\|\mathbf{z} - \mathbf{x}_k\|_2^2 + h^2\right)^{-\frac{\alpha}{2}} \mathbf{H}_k \mathbf{S}$ and ignoring the constant term $C_k^{(n)}$, the beam selector and digital precoder/combiner design problem can be equivalently rewritten as

$$\min_{\mathbf{W}, \mathbf{V}_k^H, \{\hat{s}_{i,j}\}} \sum_{k=1}^{K} \operatorname{tr}\left(C_k^{(n)} \mathbf{E}_k\right) \tag{11a}$$

$$s.t. \operatorname{tr}\left(\mathbf{Q}_k \mathbf{Q}_k^H\right) \leq P, \tag{11b}$$

$$\mathbf{Q}_k = \boldsymbol{S} \boldsymbol{W}_k, \tag{11c}$$

$$\mathbf{s}_i^T \boldsymbol{f}_j (1 - \hat{s}_{i,j}) = 0, \quad \mathbf{s}_i^T \boldsymbol{f}_j - \hat{s}_{i,j} = 0, \tag{11d}$$

$$\sum_{i=1}^{N_t} \mathbf{s}_i^T \boldsymbol{f}_j = 1, \tag{11e}$$

$$\mathbf{s}_i^T \mathbf{1} \leq 1, \quad 0 \leq \hat{s}_{i,j} \leq 1 \tag{11f}$$

where $\mathbf{E}_k$ is given by

$$\mathbf{E}_k = (\mathbf{I} - \mathbf{V}_k^H \mathbf{Q}_k)(\mathbf{I} - \mathbf{V}_k^H \mathbf{Q}_k)^H + \sigma^2 \mathbf{V}_k^H \mathbf{V}_k.$$

It is worth mentioning that the BCD type algorithms can be considered to solve the optimization problem (11), in which we divide the optimization variables into a series of subproblems. As following, the detail of the method used to solve the subproblems iteratively will be presented.

1) The Subproblem $\{\mathbf{V}_k^H\}$: We optimize the variables $\mathbf{V}_k^H$ by fixing the remaining variables. The $\mathbf{V}_k^H$ is optimized through the following problem

$$\min_{\mathbf{V}_k^H} \sum_{k=1}^{K} \operatorname{tr}\left(C_k^{(n)} \mathbf{E}_k\right) \tag{12a}$$

$$s.t. \quad \operatorname{tr}\left(\mathbf{Q}_k \mathbf{Q}_k^H\right) \leq P, \tag{12b}$$

It is a convex quadratic optimization subproblem, and this problem is subject to a quadratic constraint. By utilizing the Lagrange multiplier $\gamma > 0$ to the power constraint (12b), we can derive the optimal $\mathbf{V}_k$ can as a function of $\mathbf{Q}_k$. That is

$$\mathbf{V}_k^H \stackrel{(a)}{=} \mathbf{Q}_k^H \left((1 + \gamma)\mathbf{Q}_k \mathbf{Q}_k^H + \sigma^2 \mathbf{I}\right)^{-1}. \tag{13}$$

2) The Subproblem w.r.t. $\mathbf{W}$, $\{\overline{\mathbf{H}}_k\}$: By fixing $\{\overline{\mathbf{H}}_k\}$, the variable $\mathbf{W}$ is updated through solving the following minimization problem

$$\min_{\mathbf{W},\overline{\mathbf{H}}_k} \left\| \mathbf{Q}_k - \overline{\mathbf{H}}_k \mathbf{W} + \rho \mathbf{L}_k \right\|_F^2 \tag{14}$$

where $\mathbf{L}_k$ is the multiplier variable.

By the first-order optimality condition, the optimal $\mathbf{W}$ can be efficiently solved by a closed form. Similarly, The variable $\overline{\mathbf{H}}_k$ is updated by fixing the variable $\mathbf{W}$.

4) The Subproblem w.r.t. $\{\hat{s}_{i,j}\}$: The variable $\{\hat{s}_{i,j}\}$ can be updated with the optimization formula which fixing the remaining variables. The subproblem of optimizing $\{\hat{s}_{i,j}\}$ can be rewritten as

$$\min_{\hat{s}_{i,j}} \frac{1}{2\rho} \left(\boldsymbol{s}_i^T \boldsymbol{f}_j (1 - \hat{s}_{i,j}) + (\boldsymbol{s}_i^T \boldsymbol{f}_j - \hat{s}_{i,j}) + \rho \lambda_{i,j} \right)^2 \tag{15a}$$

$$s.t. \qquad 0 \le \hat{s}_{i,j} \le 1 \tag{15b}$$

By utilizing the first-order optimality condition, the unconstrained solution of problem (15a) is given by

$$\hat{s}_{i,j}^* = \frac{2s_{i,j}^2 + (2 + \rho\lambda_{i,j})s_{i,j} + \rho\lambda_{i,j}}{(1 + s_{i,j})^2} \tag{16}$$

Recalling that $\hat{s}_{i,j}$ satisfies $0 \le \hat{s}_{i,j} \le 1$, the optimal solution of the constrained problem (15) can be easily found in the following form

$$s_{i,j}^* = \begin{cases} 1, & 1 \le \hat{s}_{i,j}^* \\ \hat{s}_{i,j}^*, & 0 < \hat{s}_{i,j}^* < 1 \\ 0, & \hat{s}_{i,j}^* < 0 \end{cases} \tag{17}$$

5) The Subproblem w.r.t. $\{\mathbf{Q}_k\}$: The variables $\{\mathbf{Q}_k\}$ can be updated after solving the optimization problem following

$$\min_{\mathbf{Q}_k} \sum_{k=1}^{K} \left(\mathcal{C}_k^{(n)} \mathbf{E}_k \right) + \frac{1}{\rho} \left\| \mathbf{Q}_k - \overline{\mathbf{H}}_k \mathbf{W} + \rho \mathbf{L}_k \right\|_F^2 \tag{18}$$

$$s.t. \quad \mathrm{tr}\left(\mathbf{Q}_k \mathbf{Q}_k^H\right) \le P,$$

By attaching a Lagrange multiplier $\eta \ge 0$ to the power constraint and then using the KKT condition, the closed-form solution of the optimal $\mathbf{Q}_k$ is given by

$$\mathbf{Q}_k = \left(\mathbf{I} + 2\rho\eta \mathbf{V}_k \mathbf{V}_k^H + 2\rho \mathbf{V}_k \mathcal{C}_k^{(n)} \mathbf{V}_k^H \right)^{-1}$$
$$\times \left(\mathbf{B}_k + 2\rho \mathbf{V}_k (\mathcal{C}_k^{(n)})^H \right) \tag{19}$$

where $\mathbf{B}_k = \left(\overline{\mathbf{H}}_k \mathbf{W} - \rho \mathbf{L}_k \right)$.

6) The Subproblem w.r.t. $\{\boldsymbol{s}_i\}$: $\{\boldsymbol{s}_i\}$ can be optimized by fixing the remaining variables. As familiar to (12), every variable can be further optimized based on the Lagrangian multiplier method. Hence, we can rewrite the subproblem of

optimizing $\{\boldsymbol{s}_i\}$ as

$$\min_{\boldsymbol{s}_i} \frac{1}{2\rho} \sum_{j=1}^{N_t^{RF}} \left(\sum_{i=1}^{N_t} \boldsymbol{s}_i^T \boldsymbol{f}_j - 1 + \rho\mu_j \right)^2$$
$$+ \frac{1}{2\rho} \sum_{i=1}^{N_t} \sum_{j=1}^{N_t^{RF}} \left(\boldsymbol{s}_i^T \boldsymbol{f}_j (1 - \hat{s}_{i,j}) + (\boldsymbol{s}_i^T \boldsymbol{f}_j - \hat{s}_{i,j}) + \rho\lambda_{i,j} \right)^2$$
$$s.t. \quad \boldsymbol{s}_i^T \mathbf{1} \le 1, i = 1, 2, ..., N_t, \tag{20}$$

The multiplier variables $\{\boldsymbol{L}_k\}$, $\{\lambda_{i,j}\}$ and $\{\mu_j\}$ are updated as follows

$$\boldsymbol{L}_k^{(n+1)} = \boldsymbol{L}_k^{(n)} + \frac{1}{\rho^{(n)}} \left(\boldsymbol{Q}_k - \boldsymbol{SW}_k \right), \tag{21a}$$

$$\lambda_{i,j}^{(n+1)} = \lambda_{i,j}^{(n)} + \frac{1}{\rho^{(n)}} \left(\boldsymbol{s}_i^T \boldsymbol{f}_j (2 - \hat{s}_{i,j}) - \hat{s}_{i,j} \right), \tag{21b}$$

$$\mu_j^{(n+1)} = \mu_j^{(n)} + \frac{1}{\rho^{(n)}} \left(\sum_{i=1}^{N_t} (\boldsymbol{s}_i^T \mathbf{1} - 1) \right) \tag{21c}$$

It is clear that the optimization problem (20) associated with each $\boldsymbol{s}_i$ are convex with an affine constraint. By testing the first-order optimality condition, the solution of optimization problem (20) can be obtained. Finally, the beam selector $\mathbf{S}$ can be solved by using the one-iteration BCD method, which is summarized in Algorithm 1.

Algorithm 1 Solving (20) by BCD algorithm

1: **For**: $i = 1, ..., N_t$.
2:      Update the $\boldsymbol{s}_i$ according to (20);
3:      Assign $\boldsymbol{s}_i$ to the i-th row of $\mathbf{S}$;
4: **End For**

Algorithm 2 The hybrid beamforming for UAV-Enabled mmWave beamspace communication system

---

1: **Input**: the maximum transmit power P_k, and channel $\mathbf{H}_k$ for $1 \le k \le K$.
2: **Initialization**: $n = 1$, $\mathcal{K} = \{1, 2, ..., K\}$, primal variables $\{\mathbf{V}_k, \mathbf{W}, \overline{\mathbf{H}}_k, \mathbf{Q}_k, \hat{s}_{i,j}, s_j\}$, dual variables $\left\{ \mathbf{L}_k^{(n)}, \lambda_{i,j}^{(n)}, \mu_j^{(n)}, \rho^{(n)} \right\}$;
3: **while** termination condition is not reached **do**
4:      Update the altitude of UAV h according to (7);
5:      Update $\{\mathbf{V}_k\}$ according to (13);
6:      Update $\mathbf{W}$, $\{\overline{\mathbf{H}}_k\}$ according to (14);
7:      Update $\{\hat{s}_{i,j}\}$ according to (17);
8:      Update $\{\mathbf{Q}_k\}$ according to (19);
9:      Update $\{s_j\}$ according to (16);
10: **end while**
11: **Output** analog part $\mathbf{S}$ and digital part $\mathbf{W}$, $\mathbf{V}_k$

IV. SIMULATION RESULTS

In this section, we provided the simulation results and the performance of the proposed UAV-enabled mmWave MIMO system with the lens antenna arrays will be illustrated. We
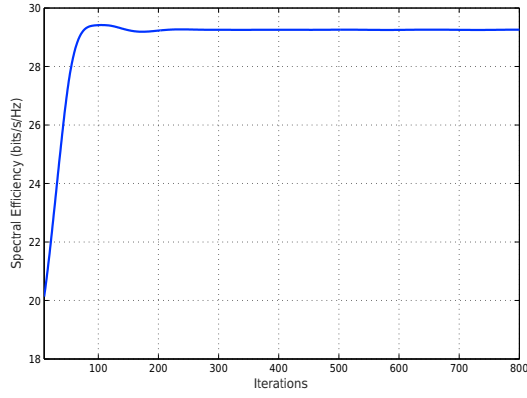
641

Fig. 2. Achievable spectral efficiency comparison versus the the number of iterations (SNR = 10 dB).
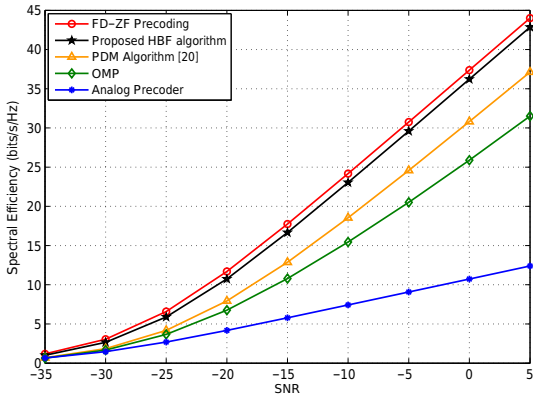

Fig. 3. Achievable spectral efficiency comparison versus the SNR.

Fig. 4. Achievable spectral efficiency comparison versus the number of users (SNR =27 dB)

will test the spectral efficiency performance of the proposed UAV-enabled mmWave beamspace MIMO scheme and make comparisons with several recent works.

Unless specified otherwise, we assume that the UAV-BS is equipped with a DLA, which consists of $N_t = 128$ antennas and $N_t^{RF} = 25$ RF chains to serve $K = 5$ GTs. The channel power gain at the reference distance $d = 1$m is $\beta_0 = -40$dB, and $\alpha = 2$ is the path-loss factor. The GTs are randomly spread within the cover of radius of 150 meters cell, such that half of the GTs are in the cover while the other GTs are placed near the cell-edge. In addition, we also set the minimum altitude of UAV $h_{\min} = 20$m, and the maximum altitude of UAV $h_{\max} = 120$m respectively.

At first, We studied the performance of the proposed algorithm on convergence, as shown in Fig. 2. In Fig. 2, we show the value of the spectral efficiency versus the number of iterations for the proposed algorithm. It can be observed that the constraint violation reduces to a threshold $\epsilon = 10^{-4}$ in less than 80 iterations, which indicates that the solution basically satisfies the equality constraints of the problem (11c).

Next, suppose the number of RF chains is equal to that of the data streams, i.e., $N_t^{RF} = KN_s = 20$, $N_r^{RF} = N_s = 4$, we investigate the spectral efficiency. In order to compare
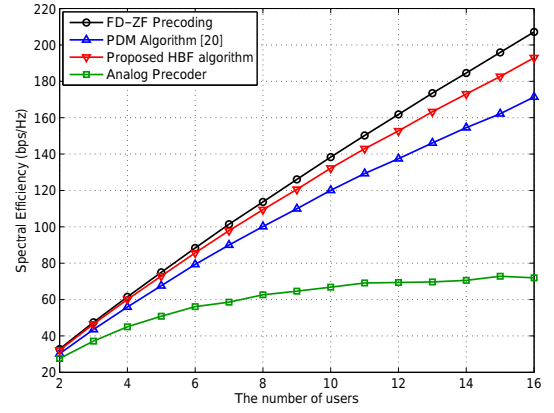
thoroughly, we simulate several classical algorithms. For comparison, the performance of the full-digital ZF precoding scheme acts as a benchmark, which is labeled by "FD-ZF" in Fig.3, and we compare the proposed algorithm with the PDM [12] and OMP algorithm [21], in order to maximize the spectral efficiency. As shown in Fig.3, the existing OMP algorithm achieves a very low spectral efficiency compare to the optimal digital precoder for the fully-connected structure. On the contrary, the optimized spectral efficiency of the proposed algorithm is close to that of the fully digital ZF precoding scheme. This implies that the proposed algorithm can accurately approximate the fully digital ZF precoding, even though the RF chains are limited.

Finally, the aforementioned schemes is analysed with different amount of GTs . In this scenario, we set $N_t = 225$, $N_t^{RF} = 25$, SNR = 27dB and the number of users K increases from 2 to 16. In Fig.4, it can be observed that except the analog precoding scheme, all the other HBF algorithms perform very close to each other under the small number of GTs. With the number of GTs increase, performances of all schemes increase monotonically. Besides, the gap between the proposed scheme performance and PDM algorithm performance escalates upon increasing number of GTs, which confirms that the proposed scheme has more potentiality under the dense GTs scenario.

Fig. 5 illustrates the spectrum efficiency of two classic precoding designs and the fully digital ZF precoding design, respectively. To obtain the statistic result, the curves are obtained by averaging over 1000 random realizations. It is observed that the proposed HBF scheme with lens achieves a superior performance improvement to the conventional analog precoding scheme. Moreover, the proposed hybrid precoders have tolerable system performance loss compared to the fully digital precoder. However, the fully digital precoder is constrained by the much higher hardware complexity, which is critical and concerned about the practical applying for mmWave communication systems.
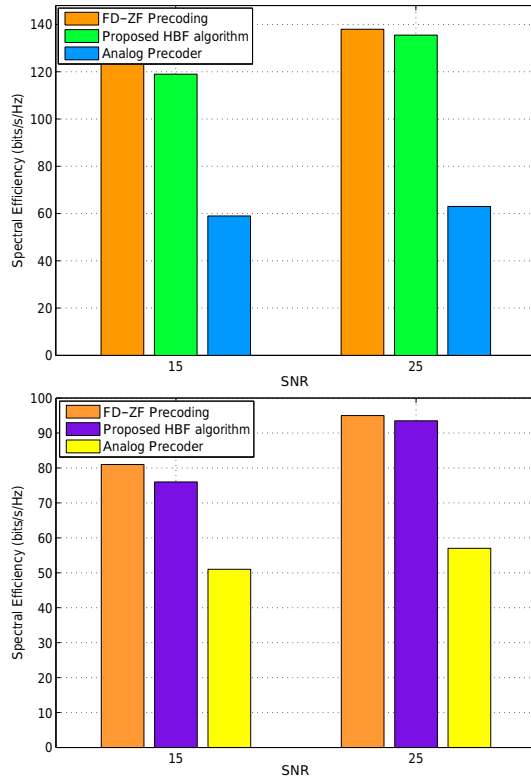
Fig. 5. Spectral efficiency comparison of the analog precoder, proposed HBF and FD-ZF Precoding (Above: $K = 10$, Below: $K = 6$).

V. CONCLUSION

In this paper, the UAV with LAAs is considered to support multi-user transmission in UAV-enabled mmWave beamspace MIMO system. In particular, we focus on jointly optimizing altitude of UAV, transmit precoder, receive combiners as well as beam selector for the sum-rate maximization problem. The original problem is a non-convex and transmit and receive variables are coupled with each other, which result in extremely strenuous to solve the proposed optimization problem. To solve this limitation, the equivalent optimization problem with the weighted MSE criterion is developed to solve the original non-convex problem. To tackle the coupling constraints problem, an efficient algorithm is proposed based on the principle of alternating optimization, which transformed the original coupling constraints problem into a series of subproblem with separable constraints. Simulation results demonstrate that the proposed algorithm could significant performance improvements over existing works in terms of SE.

REFERENCES

[1] Y. Zeng, R. Zhang, and T. J. Lim, "Wireless communications with unmanned aerial vehicles: opportunities and challenges," *IEEE Communications Magazine*, vol. 54, no. 5, pp. 36–42, 2016.

[2] W. Yi, Y. Liu, E. Bodanese, A. Nallanathan, and G. K. Karagiannidis, "A unified spatial framework for UAV-aided mmwave networks," *IEEE Transactions on Communications*, vol. 67, no. 12, pp. 8801–8817, 2019.

[3] Z. Xiao, P. Xia, and X. Xia, "Enabling UAV cellular with millimeter-wave communication: potentials and approaches," *IEEE Communications Magazine*, vol. 54, no. 5, pp. 66–73, 2016.

[4] P. Yu, W. Li, F. Zhou, L. Feng, M. Yin, S. Guo, Z. Gao, and X. Qiu, "Capacity enhancement for 5G networks using mmwave aerial base stations: Self-organizing architecture and approach," *IEEE Wireless Communications*, vol. 25, no. 4, pp. 58–64, 2018.

[5] P. V. Amadori and C. Masouros, "Low RF-complexity millimeter-wave beamspace-MIMO systems by beam selection," *IEEE Transactions on Communications*, vol. 63, no. 6, pp. 2212–2223, 2015.

[6] Y. Sun and C. Qi, "Weighted sum-rate maximization for analog beamforming and combining in millimeter wave massive MIMO communications," *IEEE Communications Letters*, vol. 21, no. 8, pp. 1883–1886, Aug. 2017.

[7] M. Artuso, D. Boviz, A. Checko, H. L. Christiansen, B. Clerckx, L. Cottatellucci, D. Gesbert, B. Gizas, A. Gopalasingham, F. Khan, J. Kelif, R. Mller, D. Ntaikos, K. Ntougias, C. B. Papadias, B. Rassouli, M. A. Sedaghat, T. Ratnarajah, L. Roullet, S. Senecal, H. Yin, and L. Zhou, "Enhancing LTE with Cloud-RAN and load-controlled parasitic antenna arrays," *IEEE Communications Magazine*, vol. 54, no. 12, pp. 183–191, 2016.

[8] B. H. Wang, H. T. Hui, and M. S. Leong, "Global and fast receiver antenna selection for MIMO systems," *IEEE Transactions on Communications*, vol. 58, no. 9, pp. 2505–2510, 2010.

[9] Y. Gao, H. Vinck, and T. Kaiser, "Massive MIMO antenna selection: Switching architectures, capacity bounds, and optimal antenna selection algorithms," *IEEE Transactions on Signal Processing*, vol. 66, no. 5, pp. 1346–1360, 2018.

[10] W. Shen, X. Bu, X. Gao, C. Xing, and L. Hanzo, "Beamspace precoding and beam selection for wideband millimeter-wave MIMO relying on lens antenna arrays," *IEEE Transactions on Signal Processing*, vol. 67, no. 24, pp. 6301–6313, 2019.

[11] M. R. Akdeniz, Y. Liu, M. K. Samimi, S. Sun, S. Rangan, T. S. Rappaport, and E. Erkip, "Millimeter wave channel modeling and cellular capacity evaluation," *IEEE Journal on Selected Areas in Communications*, vol. 32, no. 6, pp. 1164–1179, 2014.

[12] Y. Zeng and R. Zhang, "Millimeter wave MIMO with lens antenna array: A new path division multiplexing paradigm," *IEEE Transactions on Communications*, vol. 64, no. 4, pp. 1557–1571, 2016.

[13] Y. Zeng, R. Zhang, and Z. N. Chen, "Electromagnetic lens-focusing antenna enabled massive MIMO: Performance improvement and cost reduction," *IEEE Journal on Selected Areas in Communications*, vol. 32, no. 6, pp. 1194–1206, 2014.

[14] R. Guo, Y. Cai, M. Zhao, Q. Shi, B. Champagne, and L. Hanzo, "Joint design of beam selection and precoding matrices for mmwave MU-MIMO systems relying on lens antenna arrays," *IEEE Journal of Selected Topics in Signal Processing*, vol. 12, no. 2, pp. 313–325, 2018.

[15] T. Xie, L. Dai, D. W. K. Ng, and C. Chae, "On the power leakage problem in millimeter-wave massive MIMO with lens antenna arrays," *IEEE Transactions on Signal Processing*, vol. 67, no. 18, pp. 4730–4744, 2019.

[16] W. Shen, L. Dai, Y. Li, Z. Wang, and L. Hanzo, "Channel feedback codebook design for millimeter-wave massive MIMO systems relying on lens antenna array," *IEEE Wireless Communications Letters*, vol. 7, no. 5, pp. 736–739, 2018.

[17] C. Feng, W. Shen, and J. An, "Beam selection for wideband millimeter wave MIMO relying on lens antenna arrays," *IEEE Communications Letters*, vol. 23, no. 10, pp. 1875–1878, 2019.

[18] L. Liu, S. Zhang, and R. Zhang, "Multi-beam UAV communication in cellular uplink: Cooperative interference cancellation and sum-rate maximization," *IEEE Transactions on Wireless Communications*, vol. 18, no. 10, pp. 4679–4691, 2019.

[19] B. Wang, L. Dai, Z. Wang, N. Ge, and S. Zhou, "Spectrum and energy-efficient beamspace MIMO-NOMA for millimeter-wave communications using lens antenna array," *IEEE Journal on Selected Areas in Communications*, vol. 35, no. 10, pp. 2370–2382, 2017.

[20] J. Joung and Y. H. Lee, "Regularized channel diagonalization for multiuser MIMO downlink using a modified MMSE criterion," *IEEE Transactions on Signal Processing*, vol. 55, no. 4, pp. 1573–1579, 2007.

[21] O. E. Ayach, S. Rajagopal, S. Abu-Surra, Z. Pi, and R. W. Heath, "Spatially sparse precoding in millimeter wave MIMO systems," *IEEE Transactions on Wireless Communications*, vol. 13, no. 3, pp. 1499–1513, 2014.